THE JOURNAL OF PHYSICAL CHEMISTRY B

Article

pubs.acs.org/JPCB

A Light-Induced Reaction with Oxygen Leads to Chromophore Decomposition and Irreversible Photobleaching in GFP-Type Proteins

Bella L. Grigorenko,[†,‡] Alexander V. Nemukhin,*[,†,‡] Igor V. Polyakov,[†] Maria G. Khrenova,[†] and Anna I. Krylov[§]

[†]Department of Chemistry, M. V. Lomonosov Moscow State University, Leninskie Gory 1/3, Moscow, 119991, Russian Federation
[‡]N. M. Emanuel Institute of Biochemical Physics, Russian Academy of Sciences, Kosygina 4, Moscow, 119334, Russian Federation
[§]Department of Chemistry, University of Southern California, Los Angeles, California 90089-0482, United States

Supporting Information

ABSTRACT: Photobleaching and photostability of proteins of the green fluorescent protein (GFP) family are crucially important for practical applications of these widely used biomarkers. On the basis of simulations, we propose a mechanism for irreversible bleaching in GFP-type proteins under intense light illumination. The key feature of the mechanism is a photoinduced reaction of the chromophore with molecular oxygen (O_2) inside the protein barrel leading to the chromophore's decomposition. Using quantum mechanics/molecular mechanics (QM/MM) modeling we show that a model system comprising the protein-bound $Chro^-$ and O_2 can be excited to an electronic state of the intermolecular charge-transfer (CT) character ($Chro^{\bullet}\cdots O_2^{-\bullet}$). Once in the CT state, the system undergoes a series of chemical reactions with low activation barriers resulting in the cleavage of the bridging bond between the phenolic and imidazolinone rings and disintegration of the chromophore.

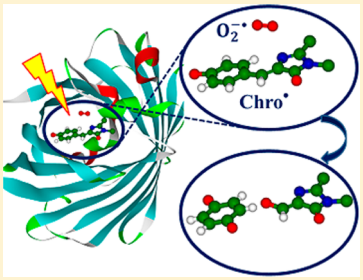

INTRODUCTION

Photobleaching, a gradual loss of optical output upon repeated irradiation, is an important process in imaging techniques using fluorescent labels.[1] Bleaching kinetics and yields depend strongly on the light source, light intensity, and other conditions, such as pH and presence of ambient oxygen and other oxidants and reducing agents. From a practical point of view, photobleaching is often considered to be a parasitic process limiting imaging applications; however, several techniques exploit photobleaching of fluorescent proteins (FPs). For example, bleaching is utilized in super-resolution imaging;[2−5] different methods based on fluorescence loss and recovery are used to track protein dynamics.[6]

Owing to its importance in practical applications, photobleaching and photostability of FPs of the green fluorescent protein (GFP) family have been extensively characterized experimentally.[1,7−16] By using a uniform protocol for measuring photostability under conditions designed to effectively simulate wide-field microscopy of live cells, Shaner et al.[1] characterized a number of FPs and concluded that in purified solutions when no oxidants are present FPs are more stable than many small-molecule fluorescent dyes. Shcherbo et al.[17] investigated the kinetics of fluorescence decay (on a time scale up to several minutes) for 10 different FPs induced by illumination by mercury arc lamps with different filters or laser lines. Dean et al.[12] studied a loss of fluorescence for several red FPs.

Despite these quantitative bleaching kinetics studies, the mechanistic understanding of photobleaching in FPs is quite rudimentary, in stark contrast to synthetic dyes.[18,19] Only a few recent studies attempted to establish a molecular-level picture of photobleaching, in particular, to relate irreversible photobleaching to structural changes of the chromophore. Pletnev et al.[10] reported a crystal structure (PDB ID: 3GL4) of the KillerRed protein[20] showing a disorder in the chromophore's region in the bleached form of the protein. The sample was obtained by 5 h of green laser light (532 nm, 5 mW) irradiation of KillerRed. Following the standard reporting protocol, the PDB entry 3GL4 lists the coordinates of all atoms including the original (i.e., undamaged) chromophore; however, the plot of electron density of the bleached form (panel B in Figure 3 of ref 10) shows no electron density in the area initially occupied by the phenolic ring. Thus, the decomposition of the chromophore in KillerRed is a hypothesis consistent with the crystallographic experiments.[10]

Almost simultaneously, Carpentier et al.[11] reported another crystal structure of the photobleached form of KillerRed (PDB ID: 2WIS) also showing a problematic assignment of the electron density in the area of the chromophore, namely, between the phenolic and imidazolinone rings. The authors proposed that the chromophore adopts a strongly tilted structure at the methyne bridge, with the phenolic ring

Received: March 9, 2015
Revised: April 12, 2015
Published: April 13, 2015

DOI: 10.1021/acs.jpcb.5b02271
J. Phys. Chem. B 2015, 119, 5444−5452

pointing into the water channel leading to the exterior of the protein.

A similar motif, sp^2-sp^3 change of the hybridization of methyne's carbon, has been observed in photobleached IrisFP under high-intensity illumination.[16] This photobleached X-ray structure shows other distortions of the protein including decarboxylation of a glutamate residue. Interestingly, a bleached structure of IrisFP obtained at low intensity irradiation[16] showed no significant changes in the chromophore, suggesting that bleaching under these conditions is due to modifications of other parts of the protein, such as sulfoxidation of cysteine and methionine.

It is not surprising that the first experimental results[10,11] revealing drastic transformations of the chromophore have been reported for KillerRed. According to the original paper[20] this fluorescent protein is particularly sensitive to photobleaching. Two special features of KillerRed should be mentioned. First, photobleaching in KillerRed is coupled with the production of toxic chemical substances. Following the very first studies,[20] the phototoxicity has been attributed to the reactive oxygen species (ROS) based on the analogy with common synthetic dyes and a strong dependence of the bleaching and the photoxicity on the presence of oxygen. Second, it has been proposed that the production and propagation of toxic species is facilitated by a water channel connecting the chromophore cavity with the exterior of the protein barrel. It was suggested that this unique structural feature of KillerRed enables the diffusion of oxygen molecules to/from the chromophore. Computer simulations[24] have illustrated that the water channel indeed increases chromophore's accessibility to oxygen.

The dependence of bleaching on oxygen concentration has also been observed in other FPs.[21−27] Several studies suggested that low photostability of some red FPs (derived from the tetrametric DsRed) might be due to the increased accessibility of the chromophore to oxygen.[25−27] In EGFP, the connection between bleaching and chromophore's accessibility to oxygen has been confirmed by mutations.[22] Whereas it is well established that oxygen plays an important role in bleaching and phototoxicity, the exact nature of phototoxic species remains unclear. References 21 and 23 reported detection of the singlet oxygen upon excitation of selected variants of FPs. Singlet oxygen has also been invoked as a key player in the IrisFP photobleaching.[16] However, a recent attempt to detect singlet oxygen in KillerRed yielded a negative result, and it was concluded that superoxide must be a primary phototoxic agent.[28]

In this work, we put forward a new mechanistic hypothesis for the irreversible photobleaching in the GFP-like proteins. By using high-level computational tools we show that the chromophore can be destroyed in a photoinduced reaction with molecular oxygen. We assume that the gateway step of bleaching is an excitation of the initial system ($Chro^-\cdots O_2$) to an intermolecular charge-transfer (CT) state. As follows from simple molecular orbital considerations,[29] electronically excited states are easier to both oxidize and reduce as compared to the ground state. Thus, the CT states can be formed by charge transfer from and to the chromophore, depending on its protonation state, hydrogen-bonding network, and local environment.

Recently, several studies have illustrated the involvement of the CT states in the FP photocycle. It has been suggested that the photoinduced decarboxylation of GFP proceeds through a state formed by CT from glutamate to the chromophore;[30,31] the existence and accessibility of such states have been later confirmed by calculations.[32,33] Charge transfer has been invoked to explain the formation of a long-lived (milliseconds) intermediate observed in several red FPs; the calculations[34] suggested that the intermediate is a dianionic $Chro^{2-}$ species formed by photoreduction of the chromophore. CT states are likely playing a role in photoinduced oxidation of FPs.[35]

Here we show that once the CT state is formed, the protein-bound $Chro^{\bullet}\cdots O_2^{-\bullet}$ radical pair can undergo a series of chemical reactions leading to the cleavage of the bridging carbon−carbon bond between the phenolic and imidazolinone rings and chromophore's decomposition. Structures and energies along the reaction pathway were computed by using a quantum mechanics/molecular mechanics (QM/MM) approach,[36] the details of which have been validated previously.[37] In our recent study,[37] this protocol has been applied to characterize the proton transfer routes in GFP. The computed structures of the A, I, and B forms of the wild-type GFP and its mutated variants were consistent with the available crystal structures, and the computed $S_0 \rightarrow S_1$ and $S_1 \rightarrow S_0$ transition energies were in excellent agreement (within 0.1 eV) with the experimental absorption and emission peaks. Thus, the protocol is suitable for interrogating chemical transformations of the GFP chromophore.

MODELS AND METHODS

QM/MM-based simulations of optical spectra of GFP-like proteins performed by several research groups[29,32,33,37−46] have demonstrated that the results are very sensitive to the subtle details of the protein structure around the chromophore. In particular, the hydrogen-bonding network connecting the chromophore and nearby amino acid residues should be correctly described. Therefore, we paid particular attention to the local structure and hydrogen-bonding network when constructing the model systems without and with the oxygen molecule near the chromophore. An initial construct without oxygen is one of the models for the wild-type GFP with the anionic chromophore considered in ref 37 among other GFP-mimicking systems. To build this model, we started from the coordinates of the relevant crystal structure of the Ser65Thr mutant of GFP (PDB ID: 1EMA),[47] restored the wild-type GFP chromophore in the anionic form, and added hydrogens. Following the manual inspection of the hydrogen bond network around the chromophore, we optimized the coordinates by using the QM/MM method as described in ref 37. To construct a system with the oxygen molecule inside the chromophore-containing pocket, we replaced the nearest to the chromophore water molecule by O_2. In all QM/MM calculations described below, the quantum subsystem comprised Chro, O_2, five water molecules, and the side chains of Arg96, Ser205, and Glu222.

We applied several computational protocols to model the photoinduced chemical transformations of the chromophore. First, the evolution of the system in the excited state in the Franck−Condon region must be examined. To trace the corresponding changes in the electronic structure, it is instructive to analyze configurational composition and orbital populations of the complete active space self-consistent field (CASSCF) wave functions. The CASSCF(8,7)/6-31G* approach in the QM-part and the AMBER force field parameters in the MM-part were used to optimize the initial structure of the model system in the ground triplet state as well

DOI: 10.1021/acs.jpcb.5b02271
J. Phys. Chem. B 2015, 119, 5444−5452

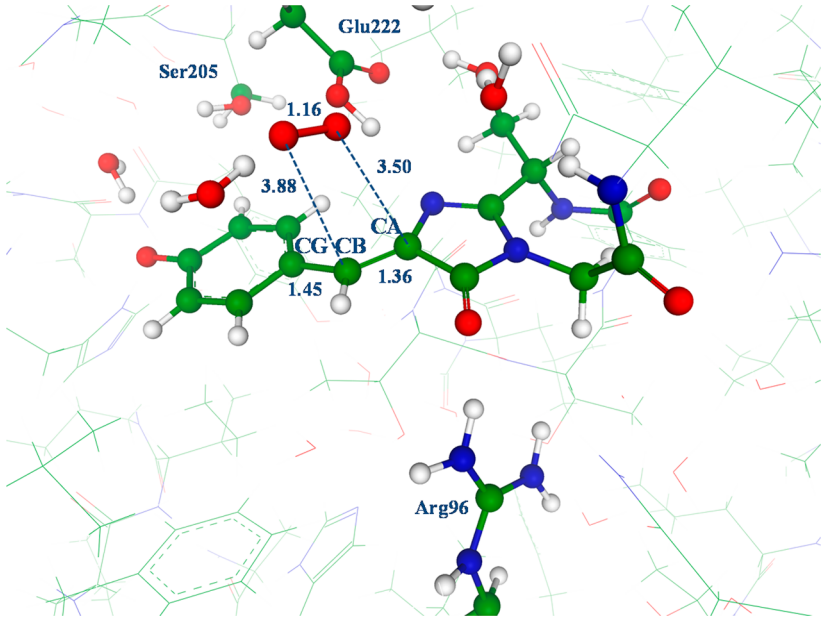

Figure 1. Equilibrium structure (computed by QM(CASSCF(8,7)/6-31G*))/MM(AMBER)) of the model system in the ground triplet state with the anionic chromophore ($Chro^-$) and molecular oxygen (O_2). The QM part is shown by balls and sticks. Here and in all figures, carbon atoms are colored in green, oxygen in red, nitrogen in blue; distances are given in Å.

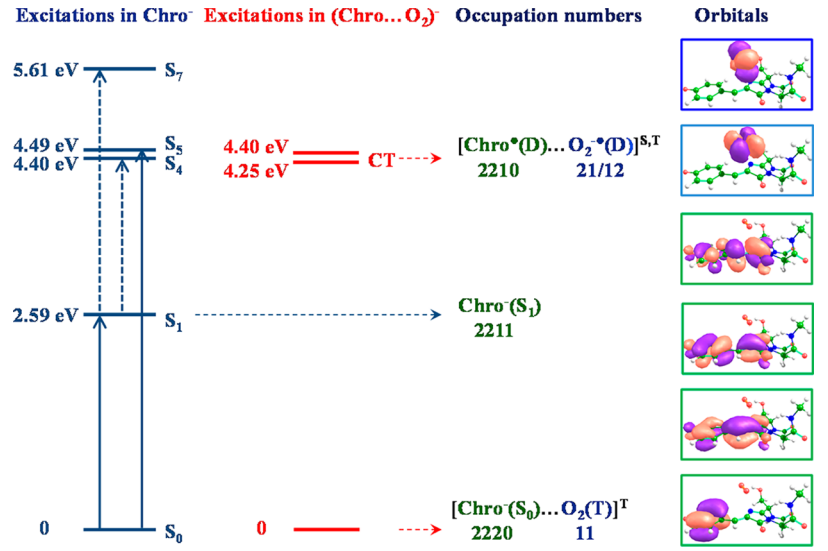

Figure 2. Left: the computed vertical excitation energies of the singlet states of GFP at the S_0 equilibrium structure. Center: the CT excited states of $(Chro{-}O_2)^-$. Right: the key active-space orbitals and their occupation numbers in the selected states. The orbitals are arranged such that the first four orbitals (counted from bottom) are localized on the chromophore and the next two are localized on O_2.

as to scan potential energy surfaces (PESs) of the triplet and singlet excited states of the intermolecular charge-transfer character. We note that CASSCF is commonly used for geometry optimization prior to calculations of electronic excitations in complex systems.[38,48] Excitation energies in the Franck–Condon region were evaluated using different QM approaches (Supporting Information contains more details), including the eXtended Multi-Configuration Quasi-Degenerate Perturbation Theory of the second order (XMCQDPT2),[49] an advanced quantum chemical method for excited states of organic fluorophores (e.g., see ref 50).

As described in Results, the evolution of the system in the CT state ultimately leads to a photooxygenated chromophore radical pair ($Chro^{\bullet}{-}O_2^{-\bullet}$) in the singlet state. From this stage onward, the reaction path was explored by using DFT in the QM subsystem. The reaction intermediates were identified as the minima on the QM(PBE0/6-31G*)/MM(AMBER) PES. The saddle points separating the reaction intermediates were located as follows: at each step of the reaction, a proper reaction coordinate was chosen (as described below), series of QM/MM constrained minimizations along such direction were carried out, and the points where the gradient changed the sign were identified. By following the steepest descent in forward and backward directions, we verified that these structures correspond to the transition states connecting the two intermediates. As in our previous work,[37] these calculations employed the effective fragment potential QM/MM variant[51] with flexible fragments.[52,53] In this scheme, molecular groups

DOI: 10.1021/acs.jpcb.5b02271
J. Phys. Chem. B 2015, 119, 5444–5452

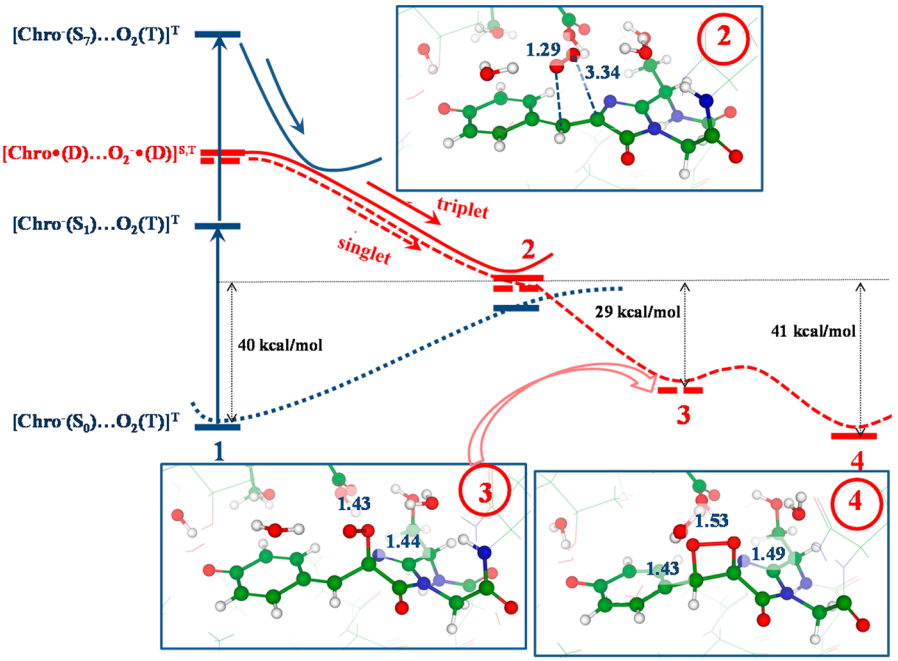

Figure 3. Possible evolution of the system from the initial structure $[Chro^{-}(S_0)\cdots O_2(T)]^T$, configuration **1** (shown in Figure 1), to the lowest-energy intermolecular CT state $[Chro^{\bullet}(D)\cdots O_2^{-\bullet}(D)]^S$, configuration **4**. Red color denotes the CT states: dashed and solid lines denote singlet and triplet states, respectively. Energies and geometries were computed by QM(CASSCF(8,7)/6-31G*)/MM(AMBER).

assigned to the MM part are represented by effective fragments contributing their one-electron potentials to the quantum Hamiltonian; the peptide chains of the protein are described as flexible unions of small effective fragments, and fragment–fragment interactions are computed with conventional force fields. The current implementation of this method enables efficient calculations of energy and energy gradients, but the evaluation of Hessian is too expensive, which precludes us from conducting standard transition-state searches.

The Cartesian coordinates of all reaction intermediates located in simulations are given in the Supporting Information.

RESULTS

Electronically Excited States in the Franck–Condon Region. As described above, we replaced one of the water molecules near the chromophore by the oxygen molecule in the model system[37] representing wt-GFP (in the anionic state) and optimized the triplet-state geometry by QM(CASSCF(8,7)/6-31G*)/MM(AMBER). Figure 1 shows the fragment of the optimized structure in which O_2 is located near the chromophore, 3.5 Å away from the CA atom of the chromophore; this is a typical distance for a π-type van der Waals complex.[54] The shape of the PES is very shallow, which is also typical for van der Waals complexes. Thus, multiple trapping sites for O_2 around the chromophore are likely to be sampled in the course of equilibrium thermal motions. Such sampling would be important for a quantitative calculation of the yield of the photoreaction; however, to illustrate the feasibility of the mechanism, this single structure is a reasonable starting point for characterizing electronic states of Chro–O_2 inside the protein barrel.

First, let us review the excited states of GFP without O_2 at the optimized geometry of the model system from ref 37. The left side in Figure 2 shows energies of the excited states (the XMCQDPT2 results) of the protein-bound anionic chromophore in the absence of oxygen as well as possible excitations with nonzero oscillator strengths. We note that although the level of the first excited state S_1 is computed fairly accurately,[37] the transition energies to higher excited states are evaluated less precisely (also, their sequential numbers may change depending on the level of theory). We see that the S_1 and S_5 states at 2.59 eV (478 nm) and 4.49 eV (276 nm) can be accessed by a one-photon excitation from S_0. The allowed transition from S_1 to S_7 is approximately at 3 eV. Based on the respective energy gaps, a nonzero oscillator strength of the S_1–S_7 transition, and a large cross section for the S_0–S_1 excitation, this state (S_7 in the current calculation) is expected to have a large two-photon absorption cross section due to resonance enhancement.

We label the states of the system composed of the chromophore and the oxygen molecule inside the protein by specifying the spin multiplicity, singlet (S), triplet (T), and doublet (D), of the entire system as well as of the chromophore and dioxygen subunits. In the latter case the assignment of the spin states to the individual moieties, Chro and O_2, cannot be carried out unambiguously; however, the orbital occupation numbers in the CASSCF wave functions allowed us to distinguish different spin states attributed to the fragments of the total system. In these notations, the initial triplet electronic state of the system composed of the anionic chromophore in the singlet state S_0 and the oxygen molecule in the triplet state $^3\Sigma_g^-$ is denoted as $[Chro^{-}(S_0)\cdots O_2(T)]^T$. Charge transfer from $Chro^-$ to O_2 gives rise to the radical-pair states $[Chro^{\bullet}(D)\cdots O_2^{-\bullet}(D)]^T$ and $[Chro^{\bullet}(D)\cdots O_2^{-\bullet}(D)]^S$, where symbol D in dioxygen refers to the $^2\Pi_g$ state of the radical anion.

As illustrated in the central part of Figure 2, the CT states corresponding to the electron transfer from $Chro^-$ to oxygen at the initial geometry (denoted **1** below, see Figure 1) lie at 4.25/4.40 eV. For this structure corresponding to relatively large separation between O_2 and Chro, the singlet and triplet radical pairs are almost degenerate. Although the exact position of the intermolecular CT states might change at a higher level of theory (see Supporting Information), we can conclude that the

DOI: 10.1021/acs.jpcb.5b02271
J. Phys. Chem. B 2015, 119, 5444–5452

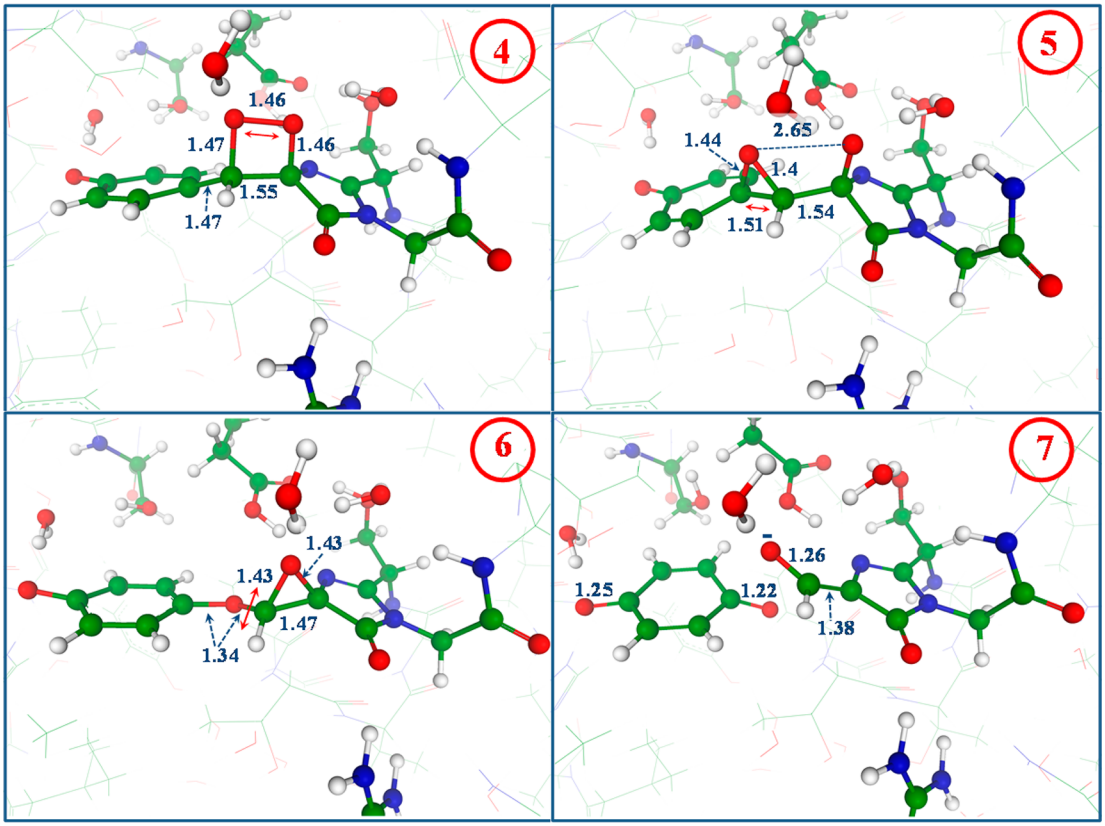

Figure 4. Reaction intermediates computed by QM(PBE0/6-31G*)/MM(AMBER).

CT states are located between S_1 and the next bright state (S_7 in our calculaton, although the sequential number of higher lying bright states may depend on the computational protocol). Our results suggest that the CT states may be accessed via radiationless relaxation either upon direct $S_0 \rightarrow S_5$ excitation (when using sufficiently short excitation wavelength) or via resonance-enhanced two-photon excitation $S_0 \rightarrow S_1 \rightarrow S_7$. The two-photon hypothesis is consistent with the fact that intense illumination conditions lead to enhanced photobleaching;[1] experimentally, such hypothesis should be verified by using high power conditions. Alternatively, the system may reach the CT state by evolving adiabatically on the $[Chro^{-}(S_1)\cdots O_2(T)]^T$ surface, similarly to the mechanism proposed in ref 33 in the context of decarboxylation.

Evolution of the System in the Charge-Transfer State. Possible evolution of the model system in the excited states (illustrated in Figure 3) was explored using the QM(CASSCF-(8,7)/6-31G*)/MM(AMBER) scheme. On the triplet-state PES $[Chro^{\bullet}(D)\cdots O_2^{-\bullet}(D)]^T$, we found a minimum energy point (intermediate **2** in Figure 3) located about 40 kcal/mol above the initial ground state structure **1**. We note that the energy of the second triplet state $[Chro^{-}(S_1)\cdots O_2(T)]^T$ is about 60 kcal/mol (2.59 eV) above the ground state.

The structure at point **2** is very similar to the initial configuration **1**, except for a stretched O−O bond in O_2 (1.29 vs 1.16 Å), which is consistent with the $O_2 \rightarrow O_2^{-\bullet}$ change in the electronic structure (the electron is attached to an antibonding MO). Also, the distances at the methyne bridge change slightly: for CA−CB 1.36 vs 1.39 Å, and CB−CG 1.45 vs 1.40 Å.

Along the valley between **1** and **2**, the energies of the singlet and triplet intermolecular CT states remain nearly degenerate. Point **2** corresponds to the minimum energy of the CT triplet state, and further evolution of the system toward lower energy structures proceeds on the singlet-state PES assuming an intersystem crossing in the vicinity of point **2**.

Starting from **2**, a slight decrease of the CA−O distance leads to the formation of intermediate **3**. Next, another C−O bond can be formed (O−CB) leading to structure **4** (Figure 3). Both reaction steps, from **2** to **3** and from **3** to **4**, require small activation energy, less than 3 kcal/mol. According to the QM(CASSCF(8,7)/6-31G*)/MM(AMBER) values, the energy of the photooxygenated product **4** is about 1 kcal/mol lower than that of initial structure **1**. Importantly, structure **4** corresponds to the lowest singlet state.

Chemical Reactions Leading to the Decomposition of the Chromophore. At this stage, we can use a DFT-based QM/MM scheme to characterize the reaction energy profile along the singlet-state PES. We employed the PBE0/6-31G* method in the QM part and the AMBER force field parameters in MM, following the protocol from our previous studies.[37] Once equilibrium structure **4** was reoptimized using QM-(PBE0/6-31G*)/MM(AMBER), we selected appropriate reaction coordinates at the consecutive steps to describe chemical transformations of the photooxygenated chromophore. Thermodynamically, this is an unstable structure, which may decompose by various channels. We considered several possible reaction pathways including those leading to the decomposition of the dioxetane motif producing carbonyl compounds.[56] Most of the channels lead to too high barriers. After many trials, we found a route with low activation barriers eventually leading to the formation of benzoquinone, as discussed below. The structures **5**, **6**, and **7** of the active site along the gradual descent along the PES are shown in panels of Figure 4.

DOI: 10.1021/acs.jpcb.5b02271
J. Phys. Chem. B 2015, 119, 5444−5452

First, we used the O−O distance in the dioxygen fragment as a reaction coordinate for the next step of the reaction. By gradually increasing this distance from the initial value of 1.46 Å and optimizing all other coordinates, we obtained the structure of the intermediate, **5**. A barrier of about 13 kcal/mol separates structures **4** and **5**; this is the highest barrier along the entire pathway, which can be overcome thermally on a millisecond time scale. We also note that, depending on the dynamical evolution in the excited state, the system might still possess some of the excess energy (the energy of the triplet CT state at the Franck−Condon geometry is about ∼100 kcal/mol higher), which can speed up the reaction.

The reaction coordinate for the next step was defined as the CG−CB distance in the chromophore (see Figure 1). A gradual increase of this distance followed by the QM/MM optimization of all other coordinates leads to intermediate **6** shown in the corresponding panel of Figure 4. The barrier between **5** and **6** is very low (around 1 kcal/mol), but the total energy drops significantly (about 38 kcal/mol) at this step. The final step corresponds to the cleavage of the CB−O bond and the formation of products, the benzoquinone molecule and the enolate ion bound to the peptide backbone of the protein. This is again a very low activation energy reaction leading to the further decrease of the total energy by about 12 kcal/mol. The reaction products, the enolate ion and the benzoquinone molecule trapped inside the protein matrix, correspond to structure **7**. The computed energy profile is illustrated in Figure 5.

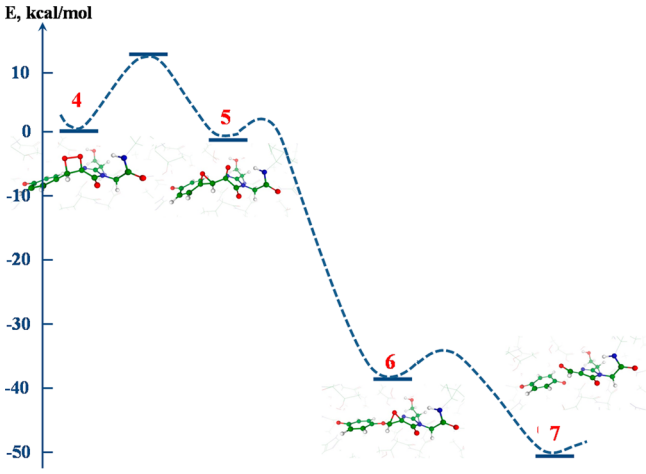

Figure 5. Energy profile computed at the QM(PBE0/6-31G*)/MM(AMBER) level of theory showing chemical destruction of the chromophore upon photooxygenation.

DISCUSSION

On the basis of the above results, we propose a tentative mechanism of photodestruction of the GFP-like chromophore in irreversible photobleaching. We showed that a model molecular system with the anionic GFP chromophore and the oxygen molecule inside the protein barrel can be excited to an intermolecular CT state ($Chro^{\bullet}\cdots O_2^{-\bullet}$). Starting from this electronic configuration, a chain of chemical reactions of $O_2^{-\bullet}$ with $Chro^{\bullet}$ leads to the destruction of the chromophore. These reactions are summarized in Figure 6. The highest activation barrier along this reaction route corresponds to 13 kcal/mol (from **4** to **5**).

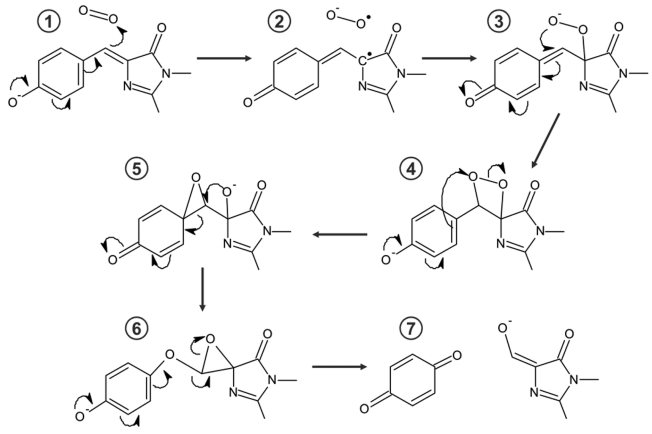

Figure 6. Chemical transformations along photoinduced reaction of the GFP chromophore with the oxygen molecule.

It should be noted that the very first step of the process, the photoinduced electron transfer from $Chro^{-}$ to O_2, is operational only if the oxygen molecule is inside the chromophore-containing pocket interacting with the π-electron system of the chromophore. There is considerable experimental evidence[20−23] that oxygen plays an important role in photobleaching and is likely able to penetrate the barrel. More importantly, the computational studies[24,25] have illustrated that oxygen can diffuse in and out of the barrel. In particular, ref 24, in which oxygen diffusion in KillerRed was investigated, has shown that although the water channel in KillerRed provides the major access pathway, other oxygen diffusion routes are also operational. The interaction between O_2 and $Chro^{-}$ is rather weak, leading to a shallow PES. Thus, different trapping sites will be accessed in the course of thermal motions, leading to fluctuations in the CT state location. Thus, our estimate of the CT state location only illustrates that these states exist and should be accessible either via a two-photon process or adiabatically. Our preliminary calculations show that the energy of the CT state can be considerably lowered (even dropping below the $[Chro^{-}(S_1)\cdots O_2(T)]^{T}$ state) in the presence of water molecules solvating O_2 (see Supporting Information), meaning that these states may be easily accessible from the S_1 state, via either adiabatic evolution or a nonadiabatic transition. Thus, the water channel in KillerRed might stabilize the intermolecular CT state thus enhancing the probability of the photoinduced CT state leading to chromophore's destruction.

In this work, we considered the formation of the superoxide radical upon photoexcitation of the chromophore−oxygen complex. The superoxide radical $O_2^{-\bullet}$ has been invoked as ROS responsible for the phototoxicity of some FPs.[28] This explanation assumes that superoxide can diffuse out of the chromophore-containing pocket to react with species *outside* the protein. While this is a sensible scenario, the calculations[24] suggest that the diffusion of superoxide might be impeded by strong electrostatic interactions with positively charged side chains. Long residence time of $O_2^{-\bullet}$ inside the protein suggests high probability of reaction with the interior protein residues. Since the chromophore itself is the nearest moiety (within 3.5 Å) and is in a highly reactive radical state ($Chro^{\bullet}$), we advocate here that the reaction of superoxide with the chromophore presents a compelling alternative scenario for the fate of superoxide, that is, the reaction with the chromophore forming the dioxetane adduct. We note that formation of the adduct with the methyne bridge (rather than other unsaturated bonds

DOI: 10.1021/acs.jpcb.5b02271
J. Phys. Chem. B 2015, 119, 5444−5452

of the chromophore) is consistent with the changes in electronic structure of the chromophore upon excitation/ionization: it is the bridge where the most significant changes in electronic density occur upon excitation and one-electron oxidation.[29,56] Whereas several decomposition pathways for this thermodynamically unstable motif may be possible,[55] our calculations suggest that one likely channel leads to the formation of benzoquinone. As illustrated by our molecular dynamics simulations (see Supporting Information), the benzoquinone molecule is able to leave the chromophore-containing pocket. Although we cannot predict the exact end product of the photoreaction, our calculations provide a plausible mechanism of the chromophore destruction consistent with the crystal structure of the bleached form of the KillerRed protein[10] in which a part of the chromophore is missing (see Supporting Information). Multiple bleaching pathways may be operational, and their importance may depend on the experimental conditions. Thus, a photobleached structure in which the chromophore is not destroyed but features a strongly deformed methyne bridge[11] possibly represents an alternative end product. We note that multiple bleaching mechanisms leading to different bleached forms have been documented for IrisFP.[16]

Our finding contributes to a growing body of evidence of the importance of photoinduced CT processes in the FP photocycle. Here, we demonstrated that the anionic GFP chromophore and a nearby oxygen molecule can be excited to an intermolecular CT state ($Chro^{\bullet}\cdots O_2^{-\bullet}$) leading to superoxide formation and a subsequent reaction of $O_2^{-\bullet}$ with the chromophore. Based on the results of a recent study, the anionic chromophore may also be photoreduced, leading to a formation of long-living intermediate,[34] which might also play a role in bleaching and phototoxicity. The neutral form of the chromophore can be photoreduced by electron transfer from the side chain of Glu222 to Chro;[32] this is believed to be a gateway step leading to decarboxylation of Glu in GFP.[30,31] A similar mechanism has been described in IrisFP.[16]

CONCLUSION

Here we put forward a new mechanism of photobleaching in GFP-type proteins based on photoinduced intermolecular charge transfer. We illustrated that photoexcitation may lead to the formation of superoxide (via photoinduced electron transfer from the anionic chromophore to O_2) initiating a series of chemical reactions leading to chromophore's breakdown. The computed minimum energy profile of the photoinduced reactions of the protein-bound anionic GFP chromophore with molecular oxygen suggests a pathway leading to the cleavage of the chemical bond between the phenolic and imidazolinone rings of the chromophore. The gateway step of this mechanism is the excited state of a charge-transfer character $[Chro^{\bullet}(D)\cdots O_2^{-\bullet}(D)]^S$ that can be described as a singlet-coupled radical-pair state. Once this state is reached, a reaction leading to the chromophore−oxygen adduct occurs. The subsequent chemical transformations result in the decomposition of the chromophore.

ASSOCIATED CONTENT

Supporting Information

Calculations of the charge-transfer excited state energies, effect of solvation and the Chro−O_2 distance on the CT state energy, molecular dynamics simulations of the reaction products, maps of the electronic density of the bleached form of the KillerRed protein, and Cartesian coordinates of the quantum part in structures **1**−**7**. This material is available free of charge via the Internet at http://pubs.acs.org.

AUTHOR INFORMATION

Corresponding Author

*E-mail: anem@lcc.chem.msu.ru; anemukhin@yahoo.com.

Notes

The authors declare no competing financial interest.

ACKNOWLEDGMENTS

We thank Prof. A. Savitsky, Dr. V. Pletnev, and Dr. N. Pletneva for advice and discussion. This study was partially supported by the Program on Molecular and Cell Biology from the Russian Academy of Sciences and by the Russian Foundation for Basic Research (Project 13-03-00207). We acknowledge the use of supercomputer resources of the Lomonosov Moscow State University[57] and of the Joint Supercomputer Center of the Russian Academy of Sciences. A.I.K. acknowledges the support from the National Science Foundation via the CHE-1264018 grant. We also acknowledge the use of supercomputer resources within the XSEDE supported project TG-CHE140041.

REFERENCES

(1) Shaner, N. C.; Steinbach, P. A.; Tsien, R. Y. A Guide to Choosing Fluorescent Proteins. *Nat. Methods* **2005**, *2*, 905−909.
(2) Burnette, D. T.; Sengupta, P.; Dai, Y.; Lippincott-Schwartz, J.; Kachar, B. Bleaching/Blinking Assisted Localization Microscopy for Superresolution Imaging Using Standard Fluorescent Molecules. *Proc. Natl. Acad. Sci. U.S.A.* **2011**, *108*, 21081−21086.
(3) Tiwari, D. K.; Nagai, T. Smart Fluorescent Proteins: Innovation for Barrier-Free Superresolution Imaging in Living Cells. *Dev. Growth Differ.* **2013**, *55*, 491−507.
(4) Nienhaus, K.; Nienhaus, G. U. Fluorescent Proteins for Live-Cell Imaging with Super-Resolution. *Chem. Soc. Rev.* **2014**, *43*, 1088−1106.
(5) Hofmann, M.; Eggeling, C.; Jakobs, S.; Hell, S. W. Breaking the Diffraction Barrier in Fluorescence Microscopy at Low Light Intensities by Using Reversibly Photoswitchable Proteins. *Proc. Natl. Acad. Sci. U.S.A.* **2005**, *102*, 17565−17569.
(6) Ishikawa-Ankerhold, H. C.; Ankerhold, R.; Drummen, G. P. Advanced Fluorescent Microscopy Techniques − FRAP, FLIP, FLAP, FRET and FLIM. *Molecules* **2012**, *17*, 4047−4132.
(7) Sinnecker, D.; Voigt, P.; Hellwig, N.; Schaefer, M. Reversible Photobleaching of Enhanced Green Fluorescent Proteins. *Biochemistry* **2005**, *44*, 7085−7094.
(8) Henderson, J. N.; Ai, H. W.; Campbell, R. E.; Remington, S. J. Structural Basis for Reversible Photobleaching of a Green Fluorescent Protein Homologue. *Proc. Natl. Acad. Sci. U.S.A.* **2007**, *104*, 6672−6677.
(9) Shaner, N. C.; Lin, M. Z.; McKeown, M. R.; Steinbach, P. A.; Hazelwood, K. L.; Davidson, M. W.; Tsien, R. Y. Improving the Photostability of Bright Monomeric Orange and Red Fluorescent Proteins. *Nat. Methods* **2008**, *5*, 545−551.
(10) Pletnev, S.; Gurskaya, N. G.; Pletneva, N. V.; Lukyanov, K. A.; Chudakov, D. M.; Martynov, V. I.; Popov, V. O.; Kovalchuk, M. V.; Wlodawer, A.; Dauter, Z.; Pletnev, V. Structural Basis for Phototoxicity of the Genetically Encoded Photosensitizer KillerRed. *J. Biol. Chem.* **2009**, *284*, 32028−32039.
(11) Carpentier, P.; Violot, S.; Blanchoin, L.; Bourgeois, D. Structural Basis for the Phototoxicity of the Fluorescent Protein KillerRed. *FEBS Lett.* **2009**, *583*, 2839−2842.
(12) Dean, K. M.; Lubbeck, J. L.; Binder, J. K.; Schwall, L. R.; Jimenez, R.; Palmer, A. E. Analysis of Red-Fluorescent Proteins Provides Insight into Dark-State Conversion and Photodegradation. *Biophys. J.* **2011**, *101*, 961−969.

DOI: 10.1021/acs.jpcb.5b02271
J. Phys. Chem. B 2015, 119, 5444−5452

(13) Roy, A.; Field, M. J.; Adam, V.; Bourgeois, D. The Nature of Transient Dark States in a Photoactivatable Fluorescent Protein. *J. Am. Chem. Soc.* **2011**, *133*, 18586−18589.
(14) de Rosny, E.; Carpentier, P. GFP-Like Phototransformation Mechanisms in the Cytotoxic Fluorescent Protein KillerRed Unraveled by Structural and Spectroscopic Investigations. *J. Am. Chem. Soc.* **2012**, *134*, 18015−18021.
(15) Subach, F. M.; Verkhusha, V. V. Chromophore Transformations in Red Fluorescent Proteins. *Chem. Rev.* **2012**, *112*, 4308−4327.
(16) Duan, C.; Adam, V.; Byrdin, M.; Ridard, J.; Kieffer-Jaquinod, S.; Morlot, C.; Arcizet, D.; Demachy, I.; Bourgeois, D. Structural Evidence for a Two-Regime Photobleaching Mechanism in a Reversibly Switchable Fluorescent Protein. *J. Am. Chem. Soc.* **2013**, *135*, 15841−15850.
(17) Shcherbo, D.; Merzlyak, E. M.; Chepurnykh, T. V.; Fradkov, A. F.; Ermakova, G. V.; Solovieva, E. A.; Lukyanov, K. A.; Bogdanova, E. A.; Zaraisky, A. G.; Lukyanov, S.; Chudakov, D. M. Bright Far-Red Fluorescent Protein for Whole-Body Imaging. *Nat. Methods* **2007**, *4*, 741−746.
(18) Stennett, E. M.; Ciuba, M. A.; Levitus, M. Photophysical Processes in Single Molecule Organic Fluorescent Probes. *Chem. Soc. Rev.* **2014**, *43*, 1057−1075.
(19) Ha, T.; Tinnefeld, P. Photophysics of Fluorescent Probes for Single-Molecule Biophysics and Superresolution and Imaging. *Annu. Rev. Phys. Chem.* **2012**, *63*, 595−617.
(20) Bulina, M. E.; Chudakov, D. M.; Britanova, O. V.; Yanushevich, Y. G.; Shkrob, M. A.; Lukyanov, S.; Lukyanov, K. A. A Genetically Encoded Photosensitizer. *Nat. Biotechnol.* **2006**, *24*, 95−99.
(21) Jiménez-Banzo, A.; Nonell, S.; Hofkens, J.; Flors, C. Singlet Oxygen Photosensitization by EGFP and its Chromophore HBDI. *Biophys. J.* **2008**, *94*, 168−172.
(22) Jiménez-Banzo, A.; Ragàs, X.; Abbruzzetti, S.; Viappiani, C.; Campanini, B.; Flors, C.; Nonell, S. Singlet Oxygen Photosensitisation by GFP Mutants: Oxygen Accessibility to the Chromophore. *Photochem. Photobiol. Sci.* **2010**, *9*, 1336−1341.
(23) Ragas, X.; Cooper, L. P.; White, J. H.; Nonell, S.; Flors, C. Quantification of Photosensitized Singlet Oxygen Production by a Fluorescent Protein. *ChemPhysChem* **2011**, *12*, 161−165.
(24) Roy, A.; Carpentier, P.; Bourgeois, D.; Field, M. Diffusion Pathways of Oxygen Species in the Phototoxic Fluorescent Protein KillerRed. *Photochem. Photobiol. Sci.* **2010**, *9*, 1342−1350.
(25) Chapagain, P. P.; Regmi, C. K.; Castillo, W. Fluorescent Protein Barrel Fluctuations and Oxygen Diffusion Pathways in mCherry. *J. Chem. Phys.* **2011**, *135*, 235101.
(26) Laurent, A. D.; Mironov, V. A.; Chapagain, P. P.; Nemukhin, A. V.; Krylov, A. I. Exploring Structural and Optical properties of Fluorescent Proteins by Squeezing: Modeling High-Pressure Effects on the mStrawberry and mCherry Red Fluorescent Proteins. *J. Phys. Chem. B* **2012**, *116*, 12426−12440.
(27) Regmi, C. K.; Bhandari, Y. R.; Gerstman, B. S.; Chapagain, P. P. Exploring the Diffusion of Molecular Oxygen in the Red Fluorescent Protein mCherry Using Explicit Oxygen Molecular Dynamics Simulations. *J. Phys. Chem. B* **2013**, *117*, 2247−2253.
(28) Vegh, R. B.; Solntsev, K. M.; Kuimova, M. K.; Cho, S.; Liang, Y.; Loo, B. L.; Tolbert, L. M.; Bommarius, A. S. Reactive Oxygen Species in Photochemistry of the Red Fuorescent Protein "Killer Red". *Chem. Commun.* **2011**, *47*, 4887−4889.
(29) Bravaya, K. B.; Grigorenko, B. L.; Nemukhin, A. V.; Krylov, A. I. Quantum Chemistry Behind Bioimaging: Insights from Ab Initio Studies of Fluorescent Proteins and their Chromophores. *Acc. Chem. Res.* **2012**, *45*, 265−75.
(30) van Thor, J. J.; Gensch, T.; Hellingwerf, K. J.; Johnson, L. N. Phototransformation of Green Fluorescent Protein with UV and Visible Light Leads to Decarboxylation of Glutamate 222. *Nat. Struct. Biol.* **2002**, *9*, 37−41.
(31) Bell, A. F.; Stoner-Ma, D.; Wachter, R. M.; Tonge, P. J. Light-driven decarboxylation of wild-type green fluorescent protein. *J. Am. Chem. Soc.* **2003**, *125*, 6919−6926.
(32) Grigorenko, B. L.; Nemukhin, A. V.; Morozov, D. I.; Polyakov, I. V.; Bravaya, K. B.; Krylov, A. I. Toward Molecular-Level Characterization of Photoinduced Decarboxylation of the Green Fluorescent Protein: Accessibility of the Charge-Transfer States. *J. Chem. Theory Comput.* **2012**, *8*, 1912−1920.
(33) Ding, L.; Chung, L. W.; Morokuma, K. Reaction Mechanism of Photoinduced Decarboxylation of the Photoactivatable Green Fluorescent Protein: An ONIOM (QM:MM) Study. *J. Phys. Chem. B* **2013**, *117*, 1075−1084.
(34) Vegh, R. B.; Bravaya, K. B.; Bloch, D. A.; Bommarius, A. S.; Tolbert, L. M.; Verkhovsky, M.; Krylov, A. I.; Solntsev, K. M. Chromophore Photoreduction in Red Fuorescent Proteins is Responsible for Bleaching and Phototoxicity. *J. Phys. Chem. B* **2014**, *118*, 4527−4534.
(35) Bogdanov, A. M.; Mishin, A. S.; Yampolsky, I. V.; Belousov, V. V.; Chudakov, D. M.; Subach, F. V.; Verkhusha, V. V.; Lukyanov, S.; Lukyanov, K. A. Green Fluorescent Proteins are Light-Induced Electron Donors. *Nat. Chem. Biol.* **2009**, *5*, 459−461.
(36) Warshel, A.; Levitt, M. Theoretical Studies of Enzymic Reactions: Dielectric Electrostatic and Steric Stabilization of the Carbonium Ion in the Reaction of Lysozyme. *J. Mol. Biol.* **1976**, *103*, 227−249.
(37) Grigorenko, B. L.; Nemukhin, A. V.; Polyakov, I. V.; Morozov, D. I.; Krylov, A. I. First-Principles Characterization of the Energy Landscape and Optical Spectra of Green Fluorescent Protein along the A → I → B Proton Transfer Route. *J. Am. Chem. Soc.* **2013**, *135*, 11541−11549.
(38) Sinicropi, A.; Andruniow, T.; Ferré, N.; Basosi, R.; Olivucci, M. Properties of the Emitting State of the Green Fluorescent Protein Resolved at the CASPT2//CASSCF/CHARMM Level. *J. Am. Chem. Soc.* **2005**, *127*, 11534−11535.
(39) Hasegawa, J.-Y.; Fujimoto, K.; Swerts, B.; Miyahara, T.; Nakatsuji, H. Excited States of GFP Chromophore and Active Site Studied by the SAC-CI Method: Effect of Protein Environment and Mutations. *J. Comput. Chem.* **2007**, *28*, 2443−2452.
(40) Virshup, A. M.; Punwong, C.; Pogorelov, T. V.; Lindquist, B. A.; Ko, C.; Martínez, T. J. Photodynamics in Complex Environments: *Ab Initio* Multiple Spawning Quantum Mechanical/ Molecular Mechanical Dynamics. *J. Phys. Chem. B* **2009**, *113*, 3280−3291.
(41) Sanchez-Garcia, E.; Doerr, M.; Hsiao, Y. W.; Thiel, W. QM/MM Study of the Monomeric Red Fluorescent Protein DsRed.M1. *J. Phys. Chem. B* **2009**, *113*, 16622−16631.
(42) Sun, Q.; Doerr, M.; Li, Z.; Smith, S. C.; Thiel, W. QM/MM Studies of Structural and Energetic Properties of the Far-Red Fluorescent Protein HcRed. *Phys. Chem. Chem. Phys.* **2010**, *12*, 2450−2458.
(43) Bravaya, K. B.; Khrenova, M. G.; Grigorenko, B. L.; Nemukhin, A. V.; Krylov, A. I. Effect of Protein Environment on Electronically Excited and Ionized States of the Green Fluorescent Protein Chromophore. *J. Phys. Chem. B* **2011**, *115*, 8296−8303.
(44) Filippi, C.; Buda, F.; Guidoni, L.; Sinicropi, A. Bathochromic Shift in Green Fluorescent Protein: A Puzzle for QM/MM Approaches. *J. Chem. Theory Comput.* **2012**, *8*, 112−124.
(45) Grigorenko, B. L.; Nemukhin, A. V.; Polyakov, I. V.; Krylov, A. I. Triple-Decker Motif for Red-Shifted Fluorescent Protein Mutants. *J. Phys. Chem. Lett.* **2013**, *4*, 1643−1747.
(46) Grigorenko, B. L.; Polyakov, I. V.; Savitsky, A. P.; Nemukhin, A. V. Unusual Emitting States of the Kindling Fluorescent Protein: Appearance of the Cationic Chromophore in the GFP Family. *J. Phys. Chem. B* **2013**, *117*, 7228−7234.
(47) Ormö, M.; Cubitt, A. B.; Kallio, K.; Gross, L. A.; Tsien, R. Y.; Remington, S. J. Crystal Structure of the Aequorea Victoria Green Fluorescent Protein. *Science* **1996**, *273*, 1392−1395.
(48) Liu, F.; Liu, Y.; De Vico, L.; Lindh, R. Theoretical Study of the Chemiluminescent Decomposition of Dioxetanone. *J. Am. Chem. Soc.* **2009**, *131*, 6181−6188.
(49) Granovsky, A. A. Extended Multi-Configuration Quasi-Degenerate Perturbation Theory: The New Approach to Multi-State

DOI: 10.1021/acs.jpcb.5b02271
J. Phys. Chem. B 2015, 119, 5444−5452

Multi-Reference Perturbation Theory. *J. Chem. Phys.* **2011**, *134*, 214113/1−214113/14.
(50) Gozem, S.; Huntress, M.; Schapiro, I.; Lindh, R.; Granovsky, A.; Angeli, C.; Olivucci, M. Dynamic Electron Correlation Effects on the Excited State Potential Energy of a Retinal Chromophore Model. *J. Chem. Theory Comput.* **2012**, *8*, 4069−4080.
(51) Gordon, M. S.; Freitag, M. A.; Bandyopadhyay, P.; Jensen, J. H.; Kairys, V.; Stevens, W. J. The Effective Fragment Potential Method:A QM-Based MM Approach to Modeling Environmental Effects in Chemistry. *J. Phys. Chem. A* **2001**, *105*, 293−307.
(52) Grigorenko, B. L.; Nemukhin, A. V.; Topol, I. A.; Burt, S. K. Modeling of Biomolecular Systems with the Quantum Mechanical and Molecular Mechanical Method Based on the Effective Fragment Potential Technique: Proposal of Flexible Fragments. *J. Phys. Chem. A* **2002**, *106*, 10663−10672.
(53) Nemukhin, A. V.; Grigorenko, B. L.; Topol, I. A.; Burt, S. K. Flexible Effective Fragment QM/MM Method: Validation through the Challenging Tests. *J. Comput. Chem.* **2003**, *24*, 1410−1420.
(54) Sherrill, C. D. Energy Component Analysis of π Interactions. *Acc. Chem. Res.* **2013**, *46*, 1020−1028.
(55) Farahani, P.; Roca-Sanjuań, D.; Zapata, F.; Lindh, R. Revisiting the Nonadiabatic Process in 1,2-Dioxetane. *J. Chem. Theory Comput.* **2013**, *9*, 5404−5411.
(56) Epifanovsky, E.; Polyakov, I.; Grigorenko, B. L.; Nemukhin, A. V.; Krylov, A. I. The Effect of Oxidation on the Electronic Structure of the Green Fluorescent Protein Chromophore. *J. Chem. Phys.* **2010**, *132*, 115104.
(57) Voevodin, Vl. V.; Zhumatiy, S. A.; Sobolev, S. I.; Antonov, A. S.; Bryzgalov, P. A.; Nikitenko, D. A.; Stefanov, K. S. Practice of "Lomonosov" Supercomputer. *Open Syst. J. (Moscow)* **2012**, *7*, 36−39.

DOI: 10.1021/acs.jpcb.5b02271
J. Phys. Chem. B 2015, 119, 5444−5452